Measurement of impact pressure and bruising of apple fruit using pressure-sensitive film technique

Fei Lu [a, c], Yutaka Ishikawa [b,*], Hiroaki Kitazawa[b], Takaaki Satake[a]

[a] Graduate School of Life and Environmental Sciences, University of Tsukuba, 1-1-1, Tennodai, Tsukuba, Ibaraki 305-8572, Japan

[b] Food Packaging Laboratory, Food Engineering Division, National Food Research Institute, 2-1-12, Kannondai, Tsukuba, Ibaraki 305-8642, Japan

[c] College of Food Science, Shenyang Agricultural University, Dongling, Shenyang, Liaoning 110161, China

* Correspondence to: Yutaka Ishikawa

Address: Food Packaging Laboratory, Food Engineering Division, National Food Research Institute, 2-1-12, Kannondai, Tsukuba, Ibaraki 305-8642, Japan

Telephone: +81- 29-838-8037

Fax: +81-29-838-7996

E-mail: yishi@affrc.go.jp

Abstract

Impact pressure and bruising of apple fruit were measured by means of a pressure-sensitive film technique, in order to develop methods for assessing and predicting bruising of apples resulting from impact loads during the course of transport and handling. Results of impact tests with apples indicate that when the fruits are dropped from different heights onto different impacting surfaces, the bruise area and volume could be assessed and predicted by regression models based on the impact force obtained from the pressure-sensitive film (F_{PSF}). The coefficients of determination (R^2) for bruise area and bruise volume were found to be 0.91 and 0.95, respectively.

Keywords: Apple; Bruising; Impact; Contact pressure; Pressure-sensitive film

1. Introduction

The fruits may pass through several containers and modes of transport from the orchard to the supermarket (Van Zeebroeck et al., 2007b). During their journey, the apples experience a variety of loading schemes that may lead to damage and bruising, the two main types are being static and dynamic loading (Lewis et al., 2008). During these processes, bruising is a major source of postharvest mechanical damage (Knee and Miller, 2002), and results in problematic losses in fresh fruit; as high as 17% in Japan during 2004 (Usuda, 2006). Much research has been conducted on impact damage to apples (Holt et al., 1981, 1985; Siyami et al., 1988; Sober et al., 1990; Chen and Yazdani, 1991; Pang et al., 1992a, 1994, 1996; Studman et al., 1997; Bajema and Hyde, 1998; Menesatti et al., 2002; Acıcan et al., 2007; Jarimopas et al., 2007), using a variety of techniques, including instrumented spheres, artificial fruit, a tactile sensor, laser scanning, and ultrasonic technique.

The most widely used is the instrumented sphere (IS) (Zapp et al., 1990; Tennes et al., 1990; Pang et al., 1992b, 1994; García-Ramos et al., 2002, 2003, 2004a, 2004b, 2004c; Desmet et al., 2004; Berardinelli et al., 2001, 2006). The change of acceleration and velocity has to be interpreted in terms of damage done to real fruit (Studman, 2001). Herold et al. (1996) developed an "artificial fruit" to detect damage sources for perishable fruit and vegetables during practical harvesting and handling. This Pressure Measuring Sphere (PMS) is capable of collecting all load events involving contact with its skin that exceed a preset threshold. Herold et al. (2001) used a tactile sensor, Type Tekscan No. 5051, to study apple contact pressure distribution between apple fruits in contact with flat and curved surfaces. Rabelo et al. (2001) measured the contact area of rubber spheres and oranges compressed against rigid, flat plates laid in parallel, by using a measuring system including a transducer board on which some micro-switches were disposed in linear, radial directions, an interface device, and a microcomputer. Lewis et al. (2007) developed analytical and numerical tools to predict bruise sizes for a given drop height against a given counterface material by dynamic finite element (FE) modeling in which a laser scan of an apple was created. Lewis et al. (2008) used a novel ultrasonic technique to study apple contact areas and stresses under static loading; the results were then used to validate the output from a finite element (FE) model of an apple.

Due to its ease of application, the pressure-sensitive film technique has been widely used to study contact area and pressure in a wide range of fields (Liggins et al., 1995; Harris et al., 1999; Zdero et al., 2001; Hoffmann et al., 2005; Bachus et al., 2006). Pressure-sensitive film can be applied directly onto the impact object to assess the interface force, pressure distribution, and contact area. It is non-invasive, and therefore will not affect the contact and can be used to detect the static and dynamic loading during the transport and handling of fruits.

The present study is initiated to use the non-invasive pressure-sensitive film technique to measure the impact pressure and pressure distribution of apple fruit impact, as experienced, for example, during the course of transport and handling. The nature of the resulting bruising was also examined in order to develop a bruise-predicting model which is based on the pressure data from the pressure-sensitive film.

2. Materials and methods

2.1. Materials

All the experiments were carried out with "sannfuji" cultivar apple fruits harvested at November, 2007, from Yamagata Prefecture, Japan. They were selected for uniformity of size, ground color and firmness, as well as freedom from defects and mechanical damage. The average weight for the apples was 279.6±9.8g. The apple fruits were stored at 4°C in air until tested at May, 2008. The tested apples can be considered as not turgid, and therefore with low damage probability.

2.2. Drop test

Impact bruises were produced by dropping apples from a measured drop height on a counterface surface. Three types of impact counterface material were used to comparatively test the different apple bruises: double wall corrugated fiberboard, rubber, and wood. In this study, drop heights were 5, 10, 15, 20, 30, 40, and 50 cm. Tests were conducted at least three times for each height. Each fruit was caught after one bounce. The pressure-sensitive film was placed on the impact counterface to indicate force and pressure distribution.

2.3. The pressure-sensitive film measurements

Fuji film (Fuji Film Corporation, Japan) is currently supplied in six grades (minute, ultra super low, super low, low, medium, and high), available to cover a wide range of pressures from 0.05 MPa to 300 MPa. With the exception of high-grade film, this material consists of two sheets (the A- and C-films), both having an active layer on one surface; on the high-grade film, these layers are currently overlaid on a single sheet.

This study employed only the two-sheet film for ultra super low pressure, in which A film is coated with a microencapsulated color forming material, and C film is coated with a color developing material (Fig. 1). When used, the two films are placed with the coated (rough and opaque) surfaces facing each other. When pressure is applied on the film, microcapsules are broken, with distribution and “density” of magenta color varying with true pressure distribution and magnitude. When microcapsules are broken, their material is released and reacts with the color-developing material, thereby forming magenta color. (Fuji Film Corporation, 2009)

Through Particle Size Control (PSC) technology, microcapsules are designed to react to various degrees of pressures, releasing their color-forming material at a density that corresponds to the specific level of applied pressure. A prescale pressure graph system (FPD-9210, Fuji Film Corporation, Japan), composed of a scanner and a computer, was used to evaluate multicolor presentation of results, resulting pressure and pressure distribution, statistical data, and others. (Fuji Film Corporation, 2009)

2.4. Bruise measurement

Bruise was measured as the procedure introduced by Lewis et al. (2007). Apples were left for 24 h after dropping, for full development of bruises. Bruise areas, *BA*, were then determined by measuring the widths using a digital caliper (w_1 and w_2, as shown in Fig. 2) and assuming that the bruises were elliptical (Bollen et al, 1999):

$$BA = \frac{\pi \cdot w_1 \cdot w_2}{4} \qquad (1)$$

where, w_1, bruise width along the major axis;

w_2, bruise width along the minor axis.

Sections through bruised apples show that the bruise shape is approximately spherical above and below a contact plane, shown on the bruise shape, Fig. 2 (Schoorl and Holt, 1980). It was observed that a section through the bruise appeared to have a circular or elliptical profile. Therefore it was proposed that the bruise volume could be described as a section of a sphere or ellipsoid. In this study, the volume was calculated for an elliptical shape defined below the contact plane (point of maximum deflection of the apple during impact) (Mohsenin, 1986; Bollen et al, 1999). Observation of bruise shapes suggests that this is a reasonable approximation. Bruise volumes were then calculated using the elliptical bruise thickness method (Mohsenin, 1986). This calculation method has been compared with a range of others (Bollen et al, 1999). The bruise widths were measured by using a digital caliper. Bruise depth was measured by using a digital caliper after the bruised apple was cut perpendicular at the bruise width along the major axis. Bruise volume, BV is given by:

$$BV = \frac{\pi \cdot d}{24}\left(3w_1 \cdot w_2 + 4d^2\right) \qquad (2)$$

where, w_1 and w_2 are bruise widths along the major and minor axes, respectively; d, bruise depth.

2.5 Statistical analysis

Statistical tests were performed using the Origin software (OriginLab Corporation, USA, version 6.1). Results were expressed as means ± standard deviation (SD) for each determination. Statistical analysis was done with one-way analysis of variance. Differences at $p<0.05$ were considered to be statistically significant.

3. Results and discussion

3.1. Apple bruising

Average apple bruise areas and volumes (calculated from Eqs. (1) and (2)) after impacts against three counterface materials are shown in Fig. 3 and Fig. 4, respectively. The smallest bruise area and volume were seen with double-wall corrugated fiberboard, and the larger with rubber and wood. In the case of fruit dropping on the three impact surfaces, the bruise area (Fig. 3) and bruise volume (Fig. 4) was increased with the drop height. Changes of the bruise due to drop height were found significant different ($p<0.05$) not only between double-wall corrugated fiberboard counterface and rubber conterface, but also between double-wall corrugated fiberboard counterface and wood conterface; it was found no significant different ($p>0.05$) between rubber counterface and wood conterface. These data show that bruises differ for the different impact surfaces from the same drop height, due to the different buffer capacities of the impact materials. These data indicate the necessity to investigate the impact force or pressure between the apple and the impact surface, in order to assess and predict the apple bruise.

3.2. The pressure-sensitive film measurements

3.2.1. Image of the pressure-sensitive film

Fig. 5 shows examples of pressure-sensitive film used for apple impacts against wood materials from various drop heights. The changes in pressured area and pressure due to drop height are significant. As would be expected, pressured area increases with dropping height. In Fig. 5, the pressured areas were 398, 513, 621, 700, 787, 884, 996 mm^2 for apple impacts against wood materials from drop heights of 5, 10, 15, 20, 30, 40, and 50 cm, respectively. The contact pressure range is 0 to 0.6 MPa, and the maximum contact pressure remains at a level of around 0.5-0.6 MPa.

The pressure-sensitive film scans show that the contact pressure is the smallest at the edge; the highest is not at the center of the contact area, but at several positions in the pressured part (as shown in Fig. 5). This data differ from those of previous investigations. Ultrasonic scans show that the contact pressure is highest at the center of the contact area, falling away towards the edge (Lewis et al. 2008). Measurements with a commercial tactile sensing system carried out by Herold et al. (2001) showed that this is the case up to a certain load, but above this load the greatest pressure is at the edge of the contact area. The three techniques have obvious differences; the commercial tactile system is invasive and could not be calibrated accurately; and the commercial tactile sensing system and the ultrasonic scans both detected the static loads in the two studies mentioned above.

3.2.2. Average pressure, pressured area, and distribution

Fig. 6 shows the pressured area against drop height for impacts against the three counterface materials. In the case of fruit dropping on the three impact surfaces, the higher the drop height, the greater the pressured area observed on the pressure-sensitive film. The biggest pressured area was found in the case of the fruit dropping on the rubber impact surface, followed by wood and double-wall corrugated fiberboard.

In the case of fruit dropping on the three impact surfaces, good linear relationships were found between pressured area and drop height. The coefficients of determination (R^2) for the double wall corrugated fiberboard, rubber, and wood were 0.96, 0.97 and 0.95, respectively. When all three types of surfaces were included, the relationship between the pressure area and drop height was poorer than that of any single impact surface (R^2=0.90).

Fig. 7 shows average pressure against drop height for impacts against the three counterface materials. Compared to the pressured area results, the different results were found in the average pressure. In the case of fruit dropping on the double-wall corrugated fiberboard surfaces, the higher the drop height, the higher the average pressure observed in the pressure-sensitive film. In the case of fruit dropping on the rubber and wood surfaces, no significant changes of average pressure were found. The biggest average pressure was found in the case of the fruit dropping on the wood impact surfaces, followed by rubber and double-wall corrugated fiberboard.

Fig. 8 shows the pressured area distribution against pressure for impacts against the three counterface materials. In the case of fruit dropping on the three impact surfaces, the value of peak pressure observed was 0.5-0.6 MPa. This fits well with measurements of "Golden Delicious" apple flesh failure stress recorded by Abbott and Lu (1996) of 0.40-0.51 MPa, as well as the peak pressure measurement by Lewis et al. (2008) of 0.5 MPa. The pressure distribution ranges observed most often for the double wall corrugated fiberboard surface, rubber surface, and wood surface were 0.1-0.3, 0.2-0.4, and 0.2-0.4 MPa respectively. This indicates that the peak contact pressure may be not sufficient to assess the apple bruise; average contact pressure may have great effect on the apple bruise.

3.3. Bruise prediction models using pressured area and average pressure

As shows in Fig. 8, the maximum pressure scanned by the pressure-sensitive film did not increase with the dropping height. This data is in accord with the previous investigation by Lewis et al. (2008). Lewis et al. (2008) found that the maximum contact pressure was not increasing with applied load by using ultrasonic technique. And it was thought that the maximum value determined was that at which the apple flesh was yielding. In this study, the value of peak pressure observed was 0.5-0.6 MPa by using pressure-sensitive film technique. The pressure distribution ranges observed often for the three impact surfaces were 0.1-0.4 MPa. When all three types of surfaces were included, both the relationship between pressured area and drop height and the relationship between average pressure and drop height were poorer than those of any single impact surface. Therefore, we find that the apple bruise cannot be well assessed from only by the pressured area and the average pressure.

Fig. 9 and 10 show the bruise area-the impact force obtained from the pressure-sensitive film (F_{PSF}), along with bruise volume- the impact force obtained from the pressure-sensitive film (F_{PSF}) relationship for apple impacts against different materials (only for the bruised apple). Table 1 shows the bruise- the impact force obtained from the pressure-sensitive film (F_{PSF}) relationship fitted by linear regression equations in the case of fruit dropping on the three impact surfaces, and all three types of surface were included. The impact force obtained from the pressure-sensitive film (F_{PSF}) was calculated by the following equation:

$$F_{PSF} = A \times P \qquad (3)$$

where F_{PSF} is the impact force obtained from the pressure-sensitive film (N); A is the pressured area (mm^2); P is the average pressure (MPa).

A good linear relationship was obtained not only between the bruise area and product of the pressured area and the average pressure, but also between the bruise volume and product of the pressured area and the average pressure. The coefficients of determination (R^2) for bruise area and bruise volume were 0.91 and 0.95, respectively.

In this study, it was only wanted to demonstrate the feasibility of assessing and predicting apple bruise by means of the pressure-sensitive film technique. Therefore, only the quantitative bruise estimation was discussed; and the relationship between the bruise probability and the parameters obtained from the pressure-sensitive film should be further studied, because the probability of damage is also another important factor for evaluating the fruit damage (Garcia-Ramos et al., 2002).

The bruise prediction models may be applied by either impact energy (Studman et al., 1997; Lewis et al. 2007; Jarimopas et al., 2007) or peak contact force (Chen and Yazdani, 1991; Bajema and Hyde, 1998; Van Zeebroeck et al., 2007a; Lewis et al. 2008). The bruise prediction model including the impact energy demands a lot of experimental work. However, the peak contact force is most likely influenced by the fruit factors themselves (temperature, radius of curvature, ripeness, etc.). In order to precisely assess and predict the apple bruise due to the impact, the whole force data must be measured exactly. In this study, the results indicate that assessing the apple bruise from the pressured area, peak pressure, or average pressure is not appropriate; however, the apple bruise area and volume can be assessed very well by the impact force obtained from the pressure-sensitive film (F_{PSF}). Therefore, the impact force obtained from the pressure-sensitive film (F_{PSF}) can clearly be used as an index to assess the apple bruise due to impact loads.

4. Conclusion

In general, we have demonstrated the feasibility of assessing and predicting apple bruise by means of the pressure-sensitive film technique. Only the quantitative bruise estimation was discussed by using the pressure-sensitive film technique; Significant differences were observed in the images of pressure-sensitive film for which the apples impact against three conterface materials, including double wall corrugated fiberboard, rubber, and wood. These results showed that assessing and predicting the apple bruise from only one of the total pressured area, the average pressure, and the peak pressure is not appropriate. They also indicate that the impact force obtained from the pressure-sensitive film (F_{PSF}) can be used to assess and predict the apple bruise; the coefficients of determination (R^2) for bruise area and bruise volume were 0.91 and 0.95, respectively. Future studies will focus on the relationship between the bruise probability and the parameters obtained from the pressure-sensitive film, and assessing methods for the small apple damage by using the pressure-sensitive film technique. Apple bruise assessment and prediction during actual transport and handling, by means of the pressure-sensitive film technique should be also further studied.

References

Abbott, J.A., Lu, R., 1996. Anisotropic mechanical properties of apples. Transactions of ASAE 39(4), 1451–1459.

Acıcan, T., Alibaş, K., Özelkök, I.S., 2007. Mechanical damage to apples during transport in wooden crates. Biosystems Engineering 96(2), 239–248.

Bachus, K., DeMarco, A., Judd, K., Horwitz, D., Brodke, D., 2006. Measuring contact area, force, and pressure for bioengineering applications: Using Fuji Film and TekScan systems. Medical Engineering & Physics 28 (5), 483–488.

Bajema, R.W., Hyde, G.M., 1998. Instrumented pendulum for impact characterization of whole fruit and vegetable specimens. Transactions of ASAE 41(5), 1399–1405.

Berardinelli, A., Guarnieri, A., Phuntsho, J., 2001. Fruit damage assessment in peach packing lines. Applied Engineering in Agriculture 17(1), 57–62.

Berardinelli, A., Donati, V., Giunchi, A., Guarnieri, A., Ragni, L., 2006. Mechanical behavior and damage of Pink Lady apples. Applied Engineering in Agriculture 22(5), 707–712.

Bollen, A.F., Nguyen, H.X., Dela Rue, B.T., 1999. Comparison of methods for estimating the bruise volume of apples. Journal of Agricultural Engineering Research 74(4), 325–330.

Chen, P., Yazdani, R., 1991. Prediction of apple bruising due to impact on different surfaces. Transactions of ASAE 34(3), 956–961.

Desmet, M., Van Linden, V., Hertog, M.L.A.T.M., Verlinden, B.E., De Baerdemaeker, J., Nicolai, B.M., 2004. Instrumented sphere prediction of tomato stem-puncture injury. Postharvest Biology and Technology 34(1), 81–92.

Fuji Film Corporation, 2009. http://www.fujindt.com/products/prescale/prescale-film.asp (access date 01.08.09).

Garcia-Ramos, F.J., Barreiro, P., Ruiz-Altisent, M., Ortiz-Canavate, J., Gil-Sierra, J., Homer, I., 2002. A procedure for testing padding materials in fruit packing lines using multiple logistic regression. Transactions of ASAE 45(3), 751–757.

Garcia-Ramos, F.J., Ortiz-Canavate, J., Ruiz-Altisent, M., 2003. Reduction of mechanical damage to apples in a packing line using mechanical devices. Applied Engineering in Agriculture 19(6), 703–707.

Garcia-Ramos, F.J., Ortiz-Canavate, J., Ruiz-Altisent, M., 2004a. Analysis of the factors implied in the fruit-to-fruit impacts on packing lines. Applied Engineering in Agriculture 20(5), 671–675.

Garcia-Ramos, F.J., Ortiz-Canavate, J., Ruiz-Altisent, M.,2004b. Evaluation and correction of the mechanical aggressiveness of commercial sizers used in stone fruit packing lines. Journal of Food Engineering 63(2), 171–176.

Garcia-Ramos, F.J., Valero, C., Ruiz-Altisent, M., Ortiz-Canavate, J., 2004c. Analysis of the mechanical aggressiveness of three orange packing systems: Packing table, box filler and net filler. Applied Engineering in Agriculture 20(6), 827–832.

Harris, M. L., Morberg, P., Bruce W. J. M., Walsh, W. R., 1999. An improved method for measuring tibiofemoral contact areas in total knee arthroplasty: a comparison of K-scan sensor and Fuji film. Journal of Biomechanics 32(9), 951–958.

Herold, B., Geyer, M., Studman, C.J., 2001. Fruit contact pressure distributions–equipment. Computers and Electronics in Agriculture 32(3), 167–179.

Herold, B., Truppel, I., Siering, G., Geyer, M., 1996. A pressure measuring sphere for monitoring handling of fruit and vegetables. Computers and Electronics in Agriculture 15(1), 73–88.

Hoffmann, K., Decker, K., 2005. Inaccuracies in measurement of contact stresses due to the measuring grid of a foil sensor. 1st International Conference on Sensing Technology. Palmerston North, New Zealand, 696–699.

Holt, J.E., Schoorl, D., 1985. A theoretical and experimental analysis of the effects of suspension and road profile on bruising in multilayered apple packs. Journal of Agricultural Engineering Research 31(4), 297–308.

Holt, J.E., Schoorl, D., Lucas, C., 1981. Prediction of bruising in impacted multilayered apple packs. Transactions of ASAE 24(1), 242–247.

Knee, M., Miller, A.R., 2002. Mechanical injury. In: Knee, M. (Ed.), Fruit quality and its biological basis (pp.157–179). Sheffield Academic press, Sheffield.

Lewis, R., Yoxall, A., Canty, L.A., Romo, E.R., 2007. Development of engineering design tools to help reduce apple bruising. Journal of Food Engineering 83 (3), 356–365.

Lewis, R., Yoxall, A., Marshall, M.B., Canty, L.A., 2008. Characterising pressure and bruising in apple fruit. Wear 264(1-2), 37–46.

Liggins, A.B., Hardie, W.R., Finlay, J.B., 1995. The spatial and pressure resolution of Fuji pressure-sensitive film. Experimental Mechanics 35(2), 166–173.

Jarimopas, B., Singh, S. P., Sayasoonthorn, S., Singh, Jagjit, 2007. Comparison of package cushioning materials to protect post-harvest impact damage to apples. Packaging Technology and Science 20(5), 315–324.

Menesatti, P., Paglia, G., Solaini, S., Zanella, A., Stainer, R., Costa, C., Cecchetti, M., 2002. Non-linear Multiple Regression Models to estimate the Drop Damage Index of Fruit. Biosystems Engineering 83(3), 319–326.

Mohsenin, N.N., 1986. Physical factors of plant and animal materials. Gordon and Breach Science Publishers, New York.

Pang, D.W., Studman, C.J., Banks, N.H., 1994. Apple bruising thresholds for an instrumented sphere. Transactions of ASAE 37(3), 893–897.

Pang, D.W., Studman, C.J., Banks, N.H., Baas, P.H., 1996. Rapid Assessment of the Susceptibility of Apples to Bruising. Journal of Agricultural Engineering Research 64(1), 37–48.

Pang, W., Studman, C.J., Ward, G.T., 1992a. Bruising damage in apple-to-apple impact. Journal of Agricultural Engineering Research 52(4), 229–240.

Pang,W.L., Studman, C.J., Banks, N.H., 1992b. Analysis of damage thresholds in apple-to-apple impacts using an instrumented sphere. New Zealand Journal of Crop and Horticultural Science 20(2), 159–166.

Rabelo, G.F., Fabbro, I.M., Linares, A.W., 2001. Contact stress area measurement of spherical fruit. Proceedings of Sensors in Horticulture III, 195–200.

Schoorl D., Holt, J.E., 1980. Bruise resistance measurements in apples. Journal of Texture Studies 11(4), 389–394.

Siyami, S., Brown, G.K., Burgess, G.J., Gerrish, J.B., Tennes, B.R., Burton, C.L., Zapp, R.H., 1988. Apple impact bruise prediction models. Transactions of ASAE 31(4), 1038–1046.

Sober, S.S., Zapp, H.R., Brown, G.K., 1990. Simulated packing line impacts for apple bruise prediction. Transactions of ASAE 33(2), 629–636.

Studman, C.J., 2001. Computers and electronics in postharvest technology - a review. Computers and Electronics in Agriculture 30(1–3), 109–124.

Studman, C.J., Brown, G.K., Timm, E.J., Schulte, N.L., Vreede, M.J., 1997. Bruising on blush and non-blush sides in apple-to-apple impacts. Transactions of ASAE 40(6), 1655–1663.

Tennes, B.R., Zapp, H.R., Marshall, D.E., Armstrong, P.R., 1990. Apple handling impact data acquisition and analysis with an instrumented sphere. Journal of Agricultural Engineering Research 47, 269–276.

Usuda, H., 2006. Basic study on development of transport simulation method and damage mechanism of fruits and vegetables. PhD Dissertation, University of Tsukuba, Japan. (In Japanese with English abstract)

Van Zeebroeck, M., Van linden, V., Darius, P., De Ketelaere, B., Ramon, H., Tijskens, E., 2007a. The effect of fruit factors on the bruise susceptibility of apples. Postharvest Biology and Technology 46(1), 10–19.

Van Zeebroeck, M., Van linden, V., Ramon, H., De Baerdemaeker, J., Nicolaï, B.M., Tijskens, E., 2007b. Impact damage of apples during transport and handling. Postharvest Biology and Technology 45(2), 157–167.

Zapp, H.R., Ehlert S.H., Brown, G.K., Armstrong, P.R., Sober, S.S., 1990. Advanced Instrumented sphere (IS) for impact measurements. Transactions of ASAE 33(3), 955–960.

Zdero, R., Fenton, P. V., Rudan, J., Bryant, J. T., 2001. Fuji film and ultrasound measurement of total knee arthroplasty contact areas. The Journal of Arthroplasty 16(3), 367–375.

Figure captions

Fig. 1. Coloring mechanism of the pressure-sensitive film (Fuji Film Corporation, 2009).

Fig. 2. Elliptical bruise thickness method for bruise determination (Bollen et al, 1999). w_1 and w_2 represent bruise widths along the major and minor axes, respectively; d, bruise depth.

Fig. 3. Relationship between bruise areas and drop heights for apple impacts against different counterface.

Fig.4. Relationship between bruise volume and drop heights for apple impacts against different counterface.

Fig.5. Examples of the pressure-sensitive film used for apple impacts against wood materials from drop heights of 5 cm (a), 10 cm (b), 15 cm (c), 20 cm (d), 30 cm (e), 40 cm (f), and 50 cm (g).

Fig. 6. Relationship between pressured area and drop heights for apple impacts against different counterface.

Fig. 7. Relationship between average pressure and drop heights for apple impacts against different counterface.

Fig. 8. Pressured area distribution on contact plates of different materials, (a) Double wall corrugated fiberboard; (b) Rubber; (c) Wood.

Fig. 9. Bruise area- F_{PSF} relationship for apple impacts against different materials. (P_{PSF},the impact force obtained from the pressure-sensitive film, is calculated by Eq. (3))

Fig.10. Bruise volume-F_{PSF} relationship for apple impacts against different materials. (P_{PSF}, the impact force obtained from the pressure-sensitive film, is calculated by Eq. (3))

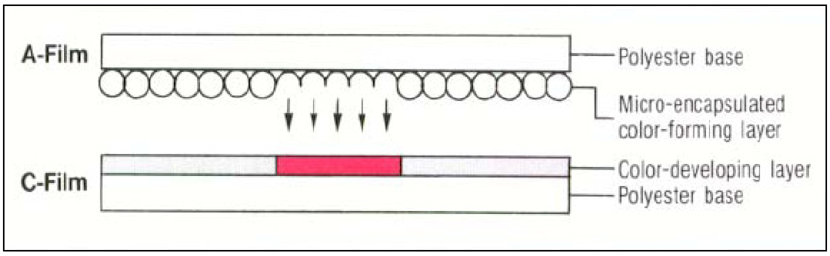

Fig. 1. Coloring mechanism of the pressure-sensitive film (Fuji Film Corporation, 2009).

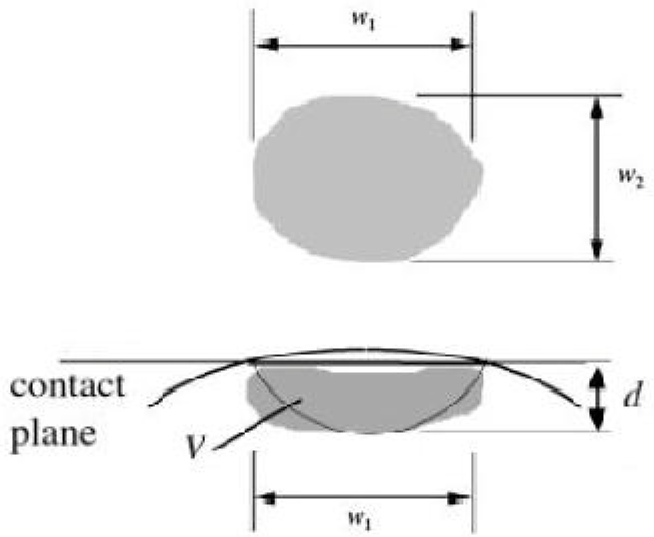

Fig. 2. Elliptical bruise thickness method for bruise determination (Bollen et al, 1999). w_1 and w_2 represent bruise widths along the major and minor axes, respectively; d, bruise depth.

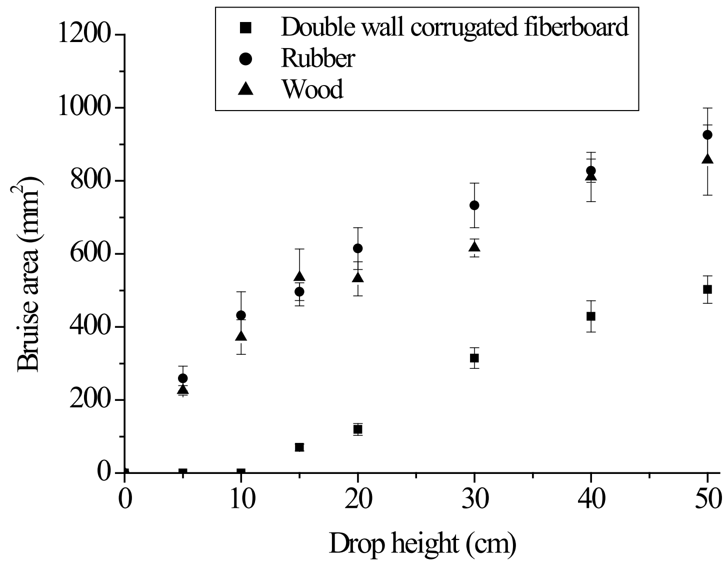

Fig. 3. Relationship between bruise areas and drop heights for apple impacts against different counterface.

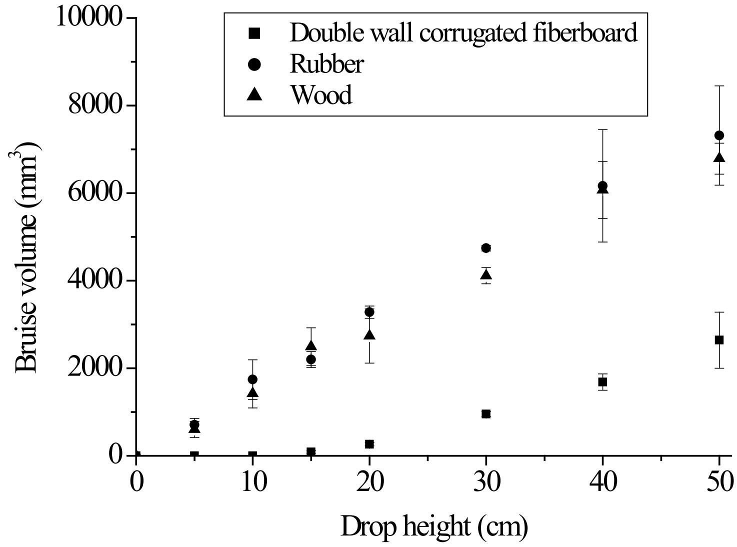

Fig.4. Relationship between bruise volume and drop heights for apple impacts against different counterface.

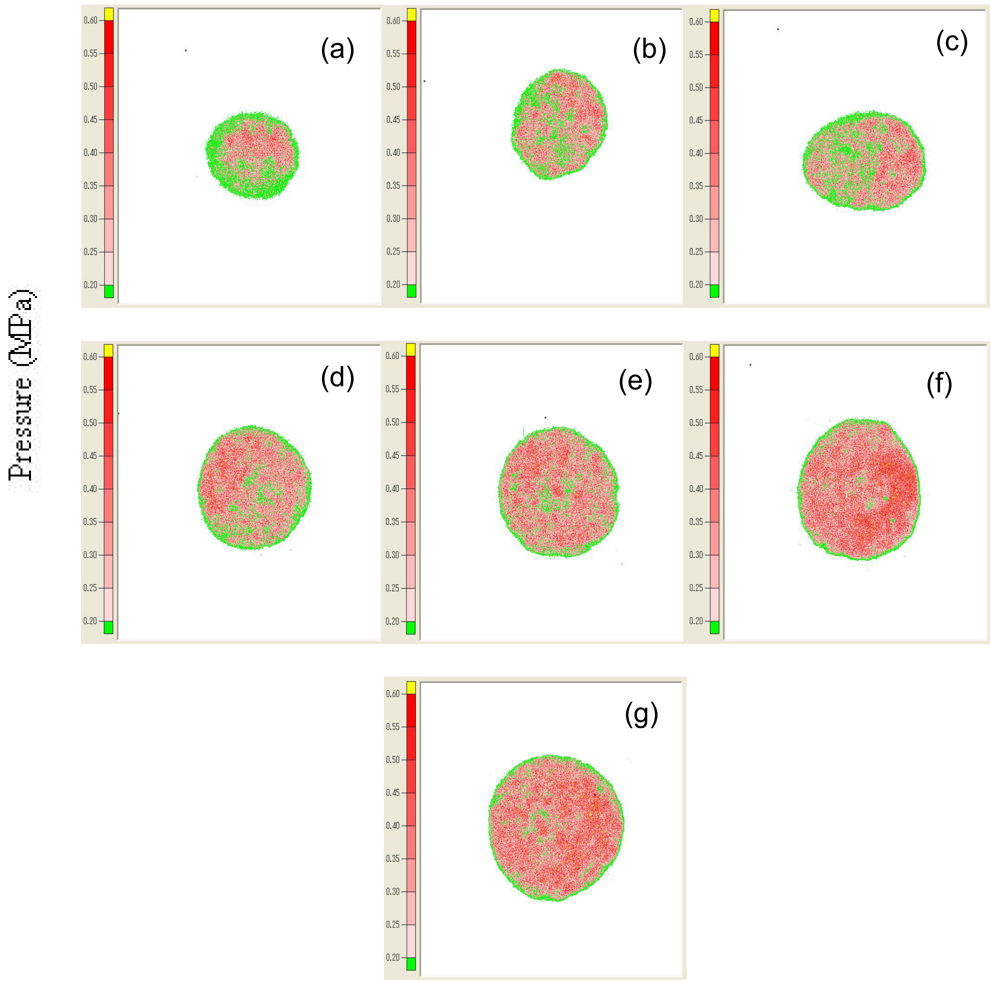

Fig.5. Examples of the pressure-sensitive film used for apple impacts against wood materials from drop heights of 5 cm (a), 10 cm (b), 15 cm (c), 20 cm (d), 30 cm (e), 40 cm (f), and 50 cm (g).

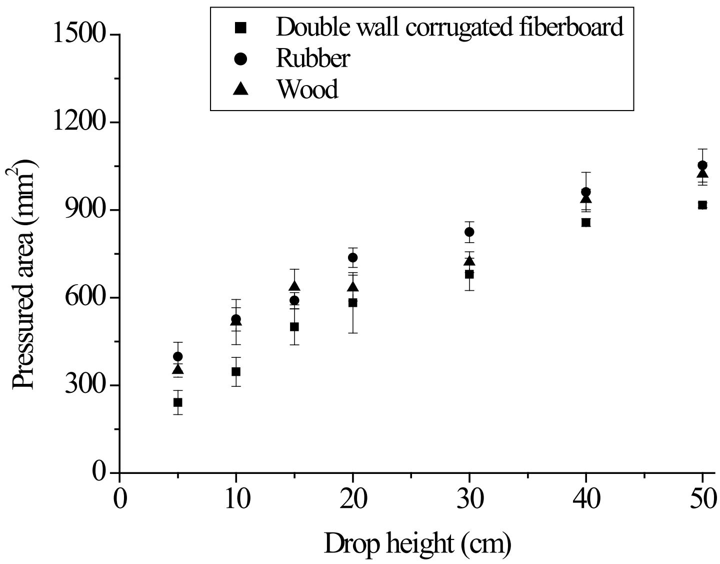

Fig. 6. Relationship between pressured area and drop heights for apple impacts against different counterface.

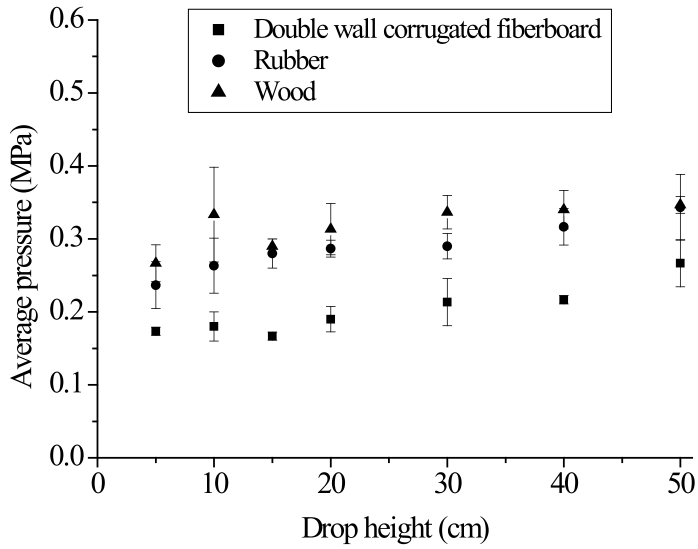

Fig. 7. Relationship between average pressure and drop heights for apple impacts against different counterface.

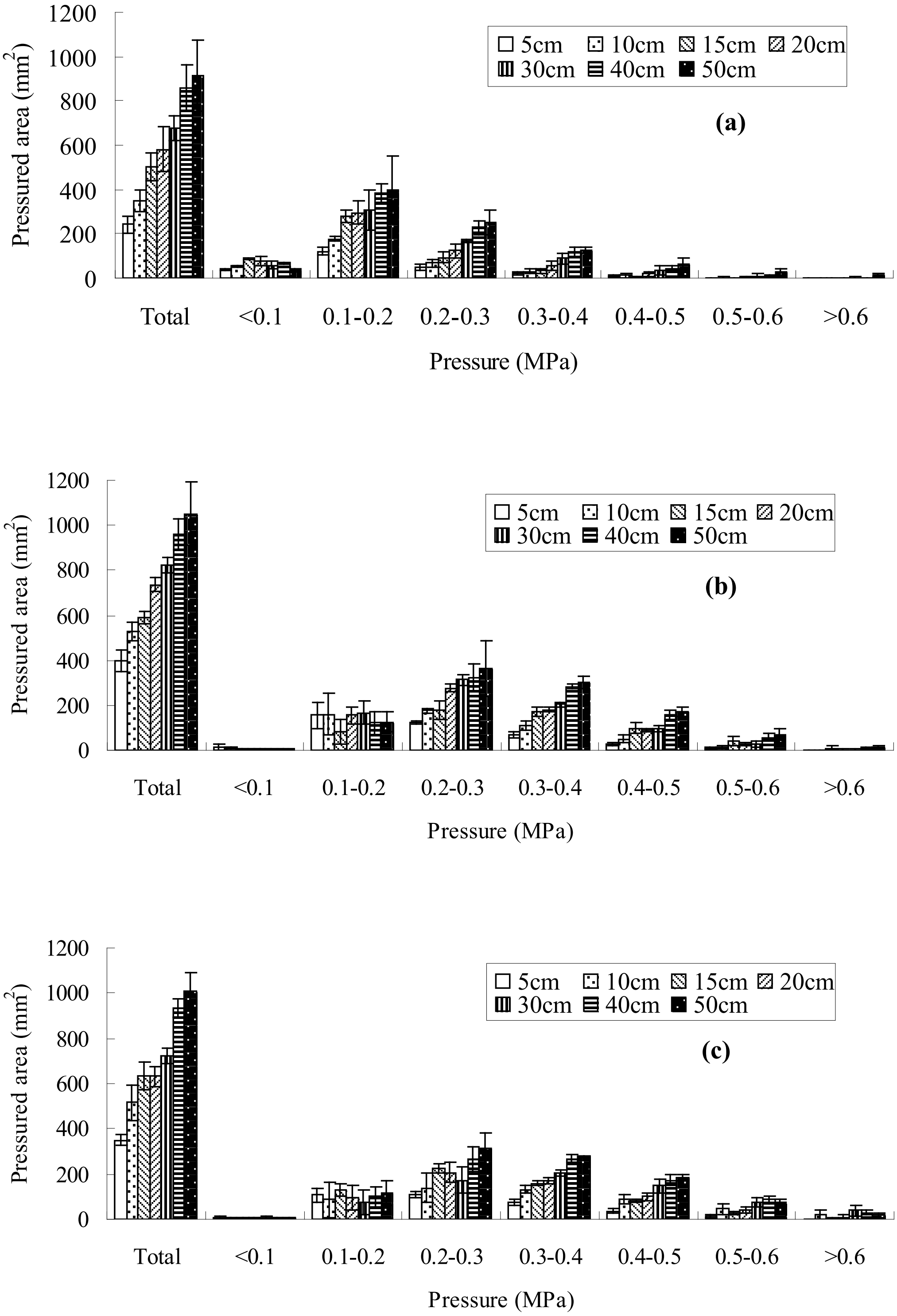

Fig. 8. Pressured area distribution on contact plates of different materials, (a) Double wall corrugated fiberboard; (b) Rubber; (c) Wood.

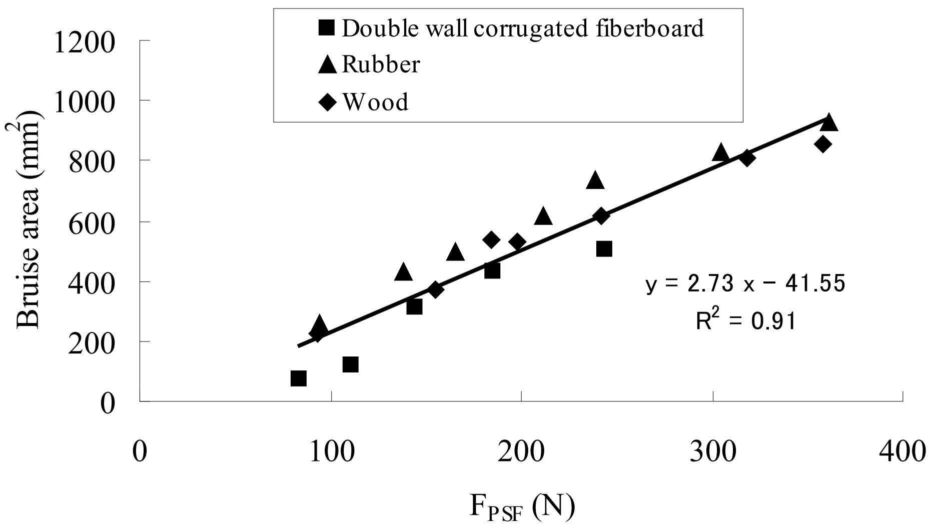

Fig. 9. Bruise area- F_{PSF} relationship for apple impacts against different materials. (P_{PSF}, the impact force obtained from the pressure-sensitive film, is calculated by Eq. (3))

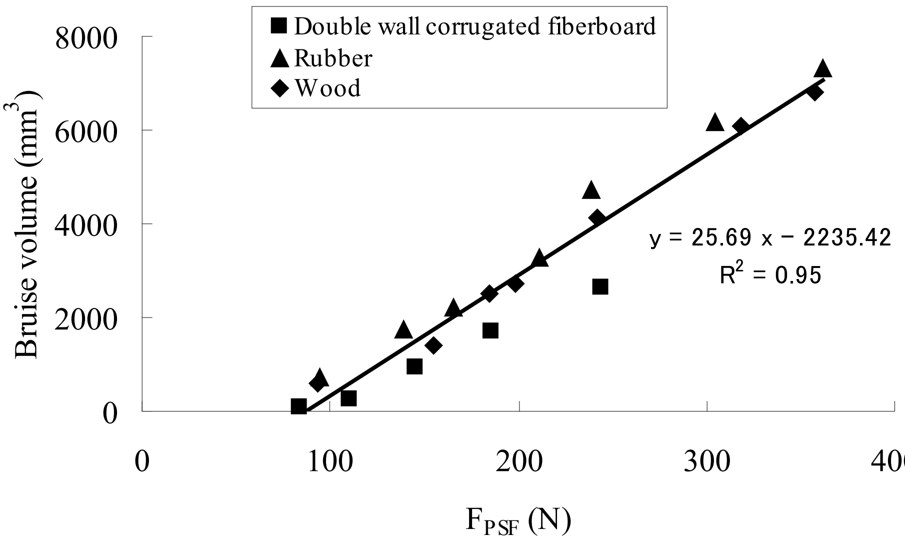

Fig.10. Bruise volume-F_{PSF} relationship for apple impacts against different materials. (P_{PSF}, the impact force obtained from the pressure-sensitive film, is calculated by Eq. (3))

Table 1. Bruise-relationship fitted by linear regression

Counterface material	Equation of relationship			
	Regression Equation	R^2	Regression Equation	R^2
Double wall corrugated fiberboard	BA=2.87×P×A-154.78	0.93	BV=16.55×P×A-1420.85	0.99
Rubber on concrete floor	BA=2.40×P×A+32.78	0.97	BV=25.73×P×A-1829.11	0.99
Wood on concrete floor	BA=2.46×P×A+79.66	0.97	BV=24.92×P×A-2055.68	0.99
Total	BA=2.73×P×A-41.55	0.91	BV=25.69×P×A-2235.42	0.95

BA, bruise area (mm^2); BV, bruise volume (mm^3); P, average pressure (MPa); A, pressured area (mm^2).